Acta Pharmaceutica Sinica B 2023;13(12):4748–4764

Chinese Pharmaceutical Association
Institute of Materia Medica, Chinese Academy of Medical Sciences

Acta Pharmaceutica Sinica B

www.elsevier.com/locate/apsb
www.sciencedirect.com

ORIGINAL ARTICLE

Preclinical and early clinical studies of a novel compound SYHA1813 that efficiently crosses the blood–brain barrier and exhibits potent activity against glioblastoma

Yingqiang Liu[a,†], Zhengsheng Zhan[b,†], Zhuang Kang[c,†], Mengyuan Li[a], Yongcong Lv[b], Shenglan Li[c], Linjiang Tong[a], Fang Feng[a], Yan Li[a], Mengge Zhang[a,f], Yaping Xue[a,f,g], Yi Chen[a,f], Tao Zhang[a], Peiran Song[a,e], Yi Su[a], Yanyan Shen[a], Yiming Sun[a], Xinying Yang[a], Yi Chen[a], Shanyan Yao[b], Hanyu Yang[d], Caixia Wang[d], Meiyu Geng[a,f], Wenbin Li[c,*], Wenhu Duan[b,*], Hua Xie[a,e,f,g,*], Jian Ding[a,f,g,*]

[a]*Division of Antitumor Pharmacology, State Key Laboratory of Drug Research, Shanghai Institute of Materia Medica, Chinese Academy of Sciences, Shanghai 201203, China*
[b]*Department of Medicinal Chemistry, Shanghai Institute of Materia Medica, Chinese Academy of Sciences, Shanghai 201203, China*
[c]*Department of Neuro-oncology, Cancer Center, Beijing Tiantan Hospital, Capital Medical University, Beijing 100070, China*
[d]*Shanghai Runshi Pharmaceutical Technology Co., Ltd., Shanghai 201218, China*
[e]*Zhongshan Institute for Drug Discovery, Shanghai Institute of Materia Medica, Chinese Academy of Sciences, Zhongshan 528400, China*
[f]*University of Chinese Academy of Sciences, Beijing 100049, China*
[g]*Hangzhou Institute for Advanced Study, University of Chinese Academy of Sciences, Hangzhou 310024, China*

Received 14 May 2023; received in revised form 30 July 2023; accepted 9 August 2023

*Corresponding authors.
E-mail addresses: jding@simm.ac.cn (Jian Ding), hxie@simm.ac.cn (Hua Xie), whduan@simm.ac.cn (Wenhu Duan), liwenbin@ccmu.edu.cn (Wenbin Li).
[†]These authors made equal contributions to this work.
Peer review under the responsibility of Chinese Pharmaceutical Association and Institute of Materia Medica, Chinese Academy of Medical Sciences.

https://doi.org/10.1016/j.apsb.2023.09.009

KEY WORDS

Small molecule inhibitor;
Glioblastoma;
VEGFR;
CSF1R;
Angiogenesis;
Macrophage;
Tumor microenvironment;
Immune-checkpoint inhibitor

Abstract Glioblastoma (GBM) is the most common and aggressive malignant brain tumor in adults and is poorly controlled. Previous studies have shown that both macrophages and angiogenesis play significant roles in GBM progression, and co-targeting of CSF1R and VEGFR is likely to be an effective strategy for GBM treatment. Therefore, this study developed a novel and selective inhibitor of CSF1R and VEGFR, SYHA1813, possessing potent antitumor activity against GBM. SYHA1813 inhibited VEGFR and CSF1R kinase activities with high potency and selectivity and thus blocked the cell viability of HUVECs and macrophages and exhibited anti-angiogenetic effects both *in vitro* and *in vivo*. SYHA1813 also displayed potent *in vivo* antitumor activity against GBM in immune-competent and immune-deficient mouse models, including temozolomide (TMZ) insensitive tumors. Notably, SYHA1813 could penetrate the blood−brain barrier (BBB) and prolong the survival time of mice bearing intracranial GBM xenografts. Moreover, SYHA1813 treatment resulted in a synergistic antitumor efficacy in combination with the PD-1 antibody. As a clinical proof of concept, SYHA1813 achieved confirmed responses in patients with recurrent GBM in an ongoing first-in-human phase I trial. The data of this study support the rationale for an ongoing phase I clinical study (ChiCTR2100045380).

1. Introduction

Glioblastoma (GBM) is the most aggressive central nervous system tumor with a median survival of 12−15 months and a less than 5% survival rate at 5 years[1]. Even with current standard-of-care treatment, mainly including surgical resection, radiation, and temozolomide (TMZ) chemotherapy, the survival of GBM patients is minimally prolonged[2,3]. Despite the apparent unmet medical need, there has been little progress in developing new treatments for GBM during the past several decades, and no small-molecule targeting agents have yet been approved for GBM treatment.

With the success of immune checkpoint therapies in the past few years, immune cells in the tumor microenvironment (TME) have become a focus of cancer research and pharmaceutical development. Tumor-associated macrophages (TAMs) are prominent microenvironment components in human GBM and play critical roles in suppressing antitumor immunity, stimulating angiogenesis, and promoting cancer cell proliferation to support tumor growth and metastasis. The abundance of TAMs in GBM is correlated with high-grade and poor disease prognosis[4,5]. Therefore, significant attention has been drawn toward the development of cancer immunotherapies targeting TAMs for GBM treatment. As the colony-stimulating factor 1 receptor (CSF1R) signaling was known to drive the recruitment of TAMs to TME and play critical roles in promoting the differentiation of TAMs toward a pro-tumorigenic M2 phenotype[6,7], inhibition of CSF1R signaling has been proposed as a promising therapeutic strategy for targeting TAM[8,9], A variety of small molecules directed at CSF1R, such as PLX3397, are in clinical development both as monotherapy and in combination with standard treatment modalities of cancer[10]. Though promising, these CSF1R inhibitors with high selectivity seem insufficient to eradicate tumors, which underscores the need for developing novel CSF1R inhibitors targeting more than one target.

Angiogenesis and vascular endothelial growth factor (VEGF) are known to play critical roles in the progression of GBM, making bevacizumab, a monoclonal antibody of VEGF-A, an essential drug in treatment regimens[11,12]. However, clinical results of bevacizumab in newly diagnosed GBM patients only showed a modest increase in progression-free survival (PFS), and no differences in overall survival were observed[13]. A large number of small-molecule inhibitors against vascular endothelial growth factor receptor (VEGFR) have been evaluated for their potential in the treatment of GBM; unfortunately, none of them showed a significant survival benefit, mainly owing to severe toxicities resulting from multi-kinase inhibition, as well as limited distribution to the brain of these inhibitors[14−16]. Thus, developing novel VEGFR-targeting agents to improve antitumor activity and reduce off-target toxicity, especially for improving brain penetrance, has gained significant attention in recent years.

Notably, TAMs have been implicated in tumor angiogenesis resistance to anti-angiogenesis therapy because TAMs represent a potent source not only for VEGF but also for several other pro-angiogenic factors[17,18]. Previous research has demonstrated macrophage depletion through CSF1R blockade overcomes adaptive resistance to anti-VEGF therapy[19,20]. Moreover, the latest study using single-cell transcriptomic profiling revealed that angiogenic signaling was enriched in PLX3397-resistant gliomas, and co-targeting of TAMs and angiogenesis decreased cell proliferation and prolonged the survival of the resistant gliomas[21]. These data support the rationale for developing novel inhibitors therapeutically co-targeting CSF1R with VEGFR, which might result in enhanced and synergistic anti-GBM activity compared with each target inhibition alone.

Here, we described the characterization of SYHA1813, a novel dual inhibitor of CSF1R and VEGFR, possessing the ability to penetrate the BBB. It exhibited potent anti-GBM activities and prolonged the survival time of mice bearing intracranial GBM, and synergistically enhanced anti-PD-1 immunotherapy. Early clinical results were described here as proof of principle.

2. Materials and methods

2.1. Compounds

SYHA1813 [6-(3-amino-1*H*-indazol-4-yl)-*N*-(4-fluoro-3-methylphenyl)-1-naphthamide] was designed and synthesized by our

research group. The purity of SYHA1813 was > 99%. For *in vitro* study, SYHA1813 was dissolved in dimethyl sulfoxide at 10 mmol/L and subsequently serially diluted to specific concentrations. For *in vivo* experiment, compound SYHA1813 was prepared as a self-microemulsion matrix and diluted to the appropriate concentration for oral administration. PLX3397 (#CSN17212) and TMZ (#CSN12046) were purchased from CSNpharm (Shanghai, China), and Axitinib (#BD114869) was purchased from LabNetwork, WuXi AppTec (Wuhan, China).

2.2. Kinase assays

VEGFR-1 (#40223) was purchased from BPS Bioscience (San Diego, CA, USA). CSF1R (#14-551), KDR (#14-630M), and VEGFR-3 (#14-681) were purchased from Millipore (MA, USA). The kinase inhibitory activity of compounds was tested using the enzyme-linked immunosorbent assay (ELISA) according to standard procedures[22]. The kinase profiling service was performed by Eurofins.

2.3. Surface plasmon resonance (SPR)

Human CSF1R (#14-551, Millipore, UK) or KDR (#10012-H20B1, Sino Biological Inc., China) protein was directly immobilized on the CM5 chip using Biacore 8K, and then the sample was used as the analyte. Use the running buffer (10 mmol/L PBS, pH 7.4, 137 mmol/L NaCl, 2.7 mmol/L KCl, 1 mmol/L $MgCl_2$, 0.05% P20, 5% DMSO) to dilute the analytes to the desired concentration, and perform multiple cycles of kinetic detection, each cycle of injection for 180 s, dissociation for 180 s. The final data were analyzed by Kinetics fitting with a 1:1 model using Biacore Insight Evaluation Software (V 2.0.15.12933). SPR was performed by Shanghai Medicilon Biopharmaceutical Co., Ltd. (Shanghai, China).

2.4. Cell lines and cell culture

U251, U87MG, and U87MG-luc cells were procured from the Cell Bank of the Chinese Academy of Sciences (Shanghai, China) and cultured in DMEM supplemented with 10% FBS. D283 was obtained from the American Type Culture Collection (ATCC, Manassas, VA, USA) and cultured in MEM containing 10% FBS, 1% NEAA, and 1% NaP. Raw264.7 was obtained from ATCC and cultured in DMEM containing 10% FBS. All cell lines were authenticated by DNA (short tandem repeat) profiling. Human umbilical vein endothelial cells (HUVEC) and endothelial cell medium (ECM, #1001) were purchased from ScienCell (San Diego, CA, USA). The mouse glioma DBT cell was obtained from the Ministry of Health Pharmaceutical Biological Products Appraisal Institute (Beijing, China) and cultured in RPMI-1640 containing 10% FBS. The mouse glioma GL261-luc cell was obtained from Cobioer biosciences Co., Ltd. (Nanjing, China) and cultured in RPMI-1640 containing 10% FBS. The preservation and culture of GL261-luc cells were conducted by Nantong Wuxi Apptec Medical Technology Co., Ltd. Bone marrow-derived macrophages (BMDM) were isolated from mouse bone marrow of BALB/c according to the standard procedure[23]. All cell lines were maintained in 5% CO_2 at 37 °C with a humidified atmosphere.

2.5. Cell viability

HUVECs were plated into 96-well plates at a density of 2500 cells per well and starved for 24 h after attachment. The compounds were added 2 h before the addition of 100 ng/mL VEGF, and the cells were incubated at 37 °C in a CO_2 incubator for 72 h. Then, the cell viability was measured using cell counting kit-8 (CCK-8) Kit (#D3100L4053, Life iLab, Shanghai, China) and multi-well spectrophotometer (VERSA max™, Molecular Devices, Sunnyvale, CA, USA) at an absorbance of 450 nm. BMDMs were isolated from mouse bone marrow and cultured for 7 days with 10 ng/mL CSF1 stimulation. Then BMDMs were plated into a 96-well culture plate at a density of 3000 cells per well and cultured overnight. The compounds were added and the cells were cultured for 72 h. The cell viability was also measured by CCK-8 Kit. GL261, DBT, D283, U87MG, and U251 cells were plated into 96-well plates and cultured overnight. Different concentrations of compounds were added, and the cells were incubated at 37 °C in a CO_2 incubator for 72 h. Then, the cell growth was measured using CCK-8 Kit. These data were collected through at least three repetitions.

2.6. Western blot

The activation of VEGFR, CSF1R, and downstream signaling molecules were examined by Western blot. After inoculating HUVEC cells in 6-well plate at a density of 2×10^5 cells per well overnight, washing them 3 times with PBS, adding 2 mL of serum-free basal medium starvation overnight, then adding gradient concentration of SYHA1813 and Axitinib for 2 h, adding VEGF factor at a final concentration of 100 ng/mL to stimulate for 15 min, discarding the culture solution, washing three times with pre-chilled PBS. Cells were lysed in SDS lysis buffer. After heating for 15 min at 100 °C, and stored at −20 °C. The newly isolated BMDM cells were seeded in 6-well plates at 2.5×10^6 cells per well, and recombinant CSF1 with a final concentration of 10 ng/mL was added. The medium was changed after 3 days of stimulation, and CSF1 stimulation was continued for 7 days. The original culture solution was discarded, and 2 mL of serum-free culture solution was added. After 6 h of starvation, different concentrations of compound SYHA1813 and PLX3397 were added for 2 h, and CSF1 with a final concentration of 50 ng/mL was added to stimulate for 15 min. After washing three times with PBS, the cells were then collected accordingly. Raw264.7 cells were seeded into six-well plates at 2×10^5 cells per well. The cells were washed three times with PBS after adherence to remove serum protein, and then, the cells were starved in the serum-free medium for 12 h. Different concentrations of SYHA1813 were added to the wells, and the cells were then incubated for 2 h before stimulation by 50 ng/mL CSF1 or 2 mL DBT conditional medium for 15 min. When Western blot analysis, whole cell lysis samples were loaded onto SDS-PAGE gels, followed by transfer to nitrocellulose membranes. Membranes were blocked with 5% milk-TBST and then blotted with primary antibodies. The following antibodies were used here: p-CSF1R (#3155S), CSF1R (#3152S), VEGFR-2 (#9698), p-AKT (#4060S), AKT (#9272S), ERK1/2 (#137F5), p-ERK1/2 (#4370), GAPDH (#5174) and Actin (#3700S) were purchased from Cell Signaling Technologies (Cambridge, MA, USA) and p-VEGFR-2 (Tyr1175) (#MA5-15170) was purchased from Thermo. The

recombinant human VEGF (#100-20-10), human CSF1 (#300-25-100) and Mouse CSF1 (#315-02-100) were purchased from Peprotech (Chicago, USA). Western blot analysis was subsequently performed with standard procedures.

Tumor tissues were lysed with RIPA (#P0013B, Beyotime, Shanghai, China) supplemented with protease inhibitor cocktail and phosphatase inhibitor (#4906837001, Roche, Basel, Switzerland). Protein concentrations were determined using a BCA protein assay kit (#23227, Thermo, MA, USA) for normalization of the samples. Equal amounts of protein were loaded on SDS-PAGE gels for blotting. Image J was used here for quantitative analysis of Western blot bands. Gray values of p-VEGFR-2 and p-CSF1R were normalized with Tubulin as the control, and then statistical analysis was conducted after three independent repetitions.

2.7. Detection of CSF1 in cell culture medium

DBT cells were seeded into six-well plates at 2×10^5 cells per well and incubated at 37 °C in a CO_2 incubator for 2 days, then the supernatant was harvested. The concentration of CSF1 in cell supernatant was detected using Mouse M-CSF ELISA Kit (#70-EK2144-96) produced by MultiSciences (Lianke) Biotech (Hangzhou, China), and DMEM medium was used as a negative control. The absorbance was read with a multiwall spectrophotometer (VERSAmax, Molecular Devices, Sunnyvale, CA, USA) at 450 nm.

2.8. The in vitro differentiation of BMDMs

The BMDM cells were plated into a 6-well culture plate at a density of 2.5×10^6 cells per well inoculated into 6-well plates in culture medium with CSF1 (10 ng/mL) for 7 days. Cells were then stimulated with 100 ng/mL CSF1, 10 ng/mL IL4 and 10 ng/mL IL13, and treated with or without PLX3397 or SYHA1813 at a final concentration of 100 nmol/L for 48 h. Flow cytometry was used to detect the expression of CD206 and ARG1 in these cells. The data were analyzed with FlowJo software (Tree Star, OR, USA). The following antibodies and cytokines were used here: recombinant mouse CSF1 (#CB34, Novoprotein, Suzhou, China), IL4 (#CK74, Novoprotein), IL13 (#CH18, Novoprotein), FVS510 (#564406, BD, New Jersey, USA), F4/80 (#565410, BD), CD11B (#563553, BD), CD206 (#25-2061-82, Thermo) and ARG1 (#46-3697-82, Thermo).

2.9. Tube formation assay

The plates were pre-coated with 60 μL growth factor reduced standard BD matrigel matrix (BD Biosciences, Billerica, MA, USA) per well and incubated at 37 °C. After being starved for 24 h, cells were plated on coated 96-well plates at 20,000 cells per well, and different concentrations of SYHA1813 and VEGF (final 100 ng/mL) were added and incubated for 8 h. Photographs were then taken through a stereoscope at 4 × magnification.

2.10. Chicken chorioallantoic membrane (CAM) assay

Fertilized chicken eggs were purchased from Shanghai Liyuan Grass-Chicken breeding Professional Cooperative. Eggs were incubated in a humidified egg incubator (Lyon Electric Company, CA, USA) that was maintained at 37 °C and 50% humidity and allowed to grow for seven days. Gentle suction was applied at the hole located at the broad end of the egg to create a false air sac directly over the chicken chorioallantoic membrane. A 1 cm^2 window was removed from the eggshell immediately afterwards. Glass coverslips (0.5 cm × 0.5 cm) saturated with SYHA1813 or vehicle control were placed on areas between preexisting vessels, and the embryos were further incubated for 48 h. The neovascular zones beside the glass coverslips were photographed under a stereomicroscope (MS5; Leica, Heerbrugg, Switzerland).

2.11. Pharmacokinetics of SYHA1813

The CD-1 mice (male) were used to study the pharmacokinetics and distribution of SYHA1813. Thirty CD-1 mice were randomly assigned into six groups corresponding to the six collection time points (0.5, 1, 2, 4, 8, and 24 h post dose) and each orally administrated with 10 mg/kg test compound. Blood samples were collected from retro orbital plexus and centrifuged to obtain plasma samples. After the intracardial perfusion treatment, brain tissue was removed from mice at designated time points. These tissues were washed with saline and dried with filter paper. Brain tissues were accurately weighed for extraction and then homogenized in MeOH-ACN (1/1, *v/v*) (5 mL/g tissue).

2.12. In vivo anti-tumor activity

2.12.1. Subcutaneous transplant model in nude mice and NOD-SCID mice

Nude mice were cultivated by the Shanghai Institute of Materia Medica, CAS (Shanghai, China). Animal experiments were performed according to the institutional ethical guidelines of animal care. U251 or U87MG Tumor cells were injected (s.c.) into the right flank of each mouse at a density of 5×10^6 cells in 200 μL PBS. When the tumor volume reached around 100 mm^3, the mice were randomly assigned to control and treatment groups ($n = 6$ for each group). Axitinib was formulated in a vehicle of 0.5% carboxymethylcellulose (#30036328, Sinopharm Chemical Reagent) and administrated once daily. SYHA1813 was orally administrated twice daily. Tumor sizes and animal weights were measured twice per week using a microcaliper and weight scale, respectively. Animals received euthanasia 17 days after administration. Tumor tissue was weighed and collected for subsequent analysis. NOD-SCID mice were purchased from HFK Bioscience (Beijing, China). Human D283 tumor cells were injected (s.c.) into the right flank of each mouse at a density of 5×10^6 in 200 μL (a mixture of 100 μL cells and 100 μL MatriGel, Croning) into NOD-SCID. When the tumor volume reached around 120 mm^3, the mice were randomly assigned to control and treatment groups ($n = 9$ each group). SYHA1813 was orally administrated twice daily. TMZ was formulated in a vehicle of 0.5% carboxymethylcellulose and orally administrated once daily. Tumor sizes and animal weights were measured three times per week using a microcaliper and weight scale, respectively. Animals received euthanasia 14 days after administration. Tumor tissue was weighed and collected for subsequent analysis.

2.12.2. Intracranial tumor model in nude mice

U87MG cell expressing luciferase (U87MG-luc) was adopted for the intracranial tumor model. After anesthetizing nude mice by intraperitoneal injection of 50 mg/kg Zoletil®50 (Virbac, France), the nude mice were placed in a prone position in the brain stereotaxic instrument, and the longitudinal incision was made at the intersection of the medial malleolus and the sagittal

midline of the head to separate the exposed skull. A hole was drilled at 2 mm to the right of the front halogen level and 0.5 mm of the skull at the front. 5×10^5 U87MG-luc cells were injected into the right striatum using a micro-pump injector in the right caudate nucleus of the naked mouse brain. The incision was sutured with sterile medical sutures and the animals were incubated until awake. Mice were randomly divided into the control group ($n = 7$), SYHA1813 40 mg/kg group ($n = 8$), SYHA1813 10 mg/kg group ($n = 8$), and Axitinib 40 mg/kg group ($n = 8$). SYHA1813 and Axitinb were orally administrated twice daily. The survival time of each mouse was recorded and the fluorescence intensity of the tumor was monitored. Luciferase-labeled GL261 (GL261-luc) cells (2×10^5) were intracranially injected into the right frontal lobes of male C57BL/6 mice aged 4−6 weeks (Beijing Vital River Laboratory Animal Technology Co., Ltd., China). The growth and quantity of xenograft tumors were monitored by bioluminescence imaging using an In Vivo Image System (IVIS) (PerkinElmer, USA). Mice were grouped at about 5 days after inoculation to measure bioluminescence and randomly grouped based on fluorescence values. Fluorescent signals in the brains of mice were measured once or twice a week. The animal experiments were conducted by Nantong Wuxi Apptec Pharmaceutical Technology Co., Ltd. In accordance with the Guide for the Care and Use of Laboratory Animals, and approved by the Institutional Animal Care and Use Committee.

2.12.3. *Subcutaneous transplant model in immunocompetent mice*

BALB/c immunocompetent mice were purchased from Lingchang Biological (Shanghai, China). Mouse glioma DBT cells were injected (s.c.) into the right flank of each mouse at a density of 5×10^6 in 200 μL PBS. When the tumor volume reached around 120 mm^3, the mice were randomly assigned into the control group, SYHA1813 10 mg/kg group ($n = 6$ each group). SYHA1813 was orally administrated twice daily. Tumor sizes and animal weights were measured three times per week. Combination with anti-PD-1 therapy in BALB/c mice. BALB/c immunocompetent mice were purchased from Lingchang Biological (Shanghai, China). Mouse glioma DBT cells were injected (s.c.) into the right flank of each mouse at a density of 3×10^6 in 100 μL PBS. When the tumor volume reached around 110 mm^3, the mice were randomly assigned to the control group, SYHA1813 5 mg/kg group, anti-PD-1 200 μg group, and combination group. There were 6 mice in each group. The rat IgG2a isotype control (#BE0089, Bio-X-cell, New Hampshire, USA) was employed in the control group. SYHA1813 was orally administrated twice daily and anti-PD-1 (#BE0146, Bio-X-cell) was administrated twice a week with intraperitoneal injection. Tumor sizes and animal weights were measured three times per week. This experiment was conducted in two batches simultaneously, with one batch terminated on Day 7 for CyTOF analysis and the other utilized to investigate changes in tumor volume. The tumor volume (V) was calculated as Eq. (1):

$$V = 0.5 \times [\text{Length (mm)} \times \text{Width}^2\ (\text{mm}^2)] \quad (1)$$

The individual relative tumor volume (RTV) was calculated as Eq. (2):

$$\text{RTV} = V_t/V_0 \quad (2)$$

where V_t is the volume on each day, and V_0 represents the volume at the beginning of the treatment.

2.13. *CyTOF analysis*

For the analysis of tumor-infiltrating immune cells, a small number of fresh and undecomposed tumor masses were selected from the tumor mass. These small tumors were quickly dissected with surgical scissors, then soaked in the prepared tumor isolation kit (#130-096-730, Miltenyi) for 1 h, then filtered and $CD45^+$ isolated using CD45 MicroBeads (#130-052-301, Miltenyi). Two million cells were taken for surface staining, CD45-89Y, CD11b-110Cd, CD3-152Sm, F4/80-146Nd, iNOS-161Dy, CD206-169 Tm, CD4-145Nd, CD25-151Eu, CD8-168Er, PDL1-153Eu, and PD1-159 Tb antibodies were added, respectively, which were purchased from Fluidigm (San Francisco, CA, USA), and incubated on ice for 30 min. Cells were suspended in Maxpar Cell Staining Buffer (CSB, Fluidigm) and labeled with 0.5 μmol/L cisplatin solution (Fluidigm) for 5 min. After adding 500 μL of Nuclear Antigen Staining Buffer (NASB), the mixture was vortexed and incubated at room temperature for 30 min. Then after 2 mL of Nuclear Antigen Staining Perm (NASP, Fluidigm) added, it was well mixed and centrifuged at $500 \times g$ for 6 min at 4 °C, and the supernatant solution was discarded, cells were resuspended by vortexing. Foxp3-158Gd and Granzyme B antibodies were then added followed by vortexing and incubation on ice for 30 min. After adding 2 mL of CSB, it was mixed well and centrifuged at $500 \times g$ for 6 min at 4 °C. The supernatant was discarded, and cells were resuspended by vortexing. Finally, 500 μL of 125 nmol/L Ir (Fluidigm) added, followed by vortexing, the samples were placed on ice for 1 h or overnight at 4 °C. The cells were then loaded onto the Helios sample loader for data acquisition. Analysis was performed with Cytobank 7.3.0 (Beckman Coulter, California, USA).

Brain tumor tissue dissociation and CyTOF analysis, mice with intracranial tumors had their brain tissue surgically removed after 9 days of administration. The tumor-bearing brain hemispheres were dissociated enzymatically to obtain a single-cell suspension with a Brain Tumor Dissociation Kit (#130-095-942, Miltenyi Biotec) according to the manufacturer's protocol. The cell suspension was filtered through a 70 μm strainer and centrifuged at $300 \times g$, 4 °C for 5 min. Next, $CD45^+$ cells were isolated using CD45 MicroBeads (#130-052-301, Miltenyi) and LS columns. Staining and analysis of CyTOF were conducted in accordance with the standard procedure descried in the preceding paragraph.

2.14. *Immunohistochemistry*

Tumor samples were fixed in formalin for over 24 h, transferred to 70% ethanol, and embedded in paraffin wax. Sections were cut and baked onto microscope slides. Immunohistochemistry was performed by Shanghai Zuocheng Biotechnology (Shanghai, China). Stained sections were imaged using a NanoZoomer S210 (C13239-01, Hamamatsu, Japan) and photos were analyzed by NDP.scan 3.2.15. The following antibodies were used here: Ki67 (#ab16667), CD206 (#ab64693), CD163 (#ab182422), CD105 (#ab221675), CD31 (#ab28364) and MIP3A (#ab9829) antibodies were purchased from Abcam (Cambridge, UK), and CD8 (#14-0808) was purchased from eBioscience (San Diego, USA). We employed the multiplicative quick score method to assess protein expression[24].

2.15. Immunofluorescence

Upon completion of the experiment, the brains tissue of mice with intracranial tumors were fixed in paraformaldehyde for 2−3 days and subsequently subjected to embedding treatment. Immunofluorescence was performed by Shanghai Zuocheng Biotechnology (Shanghai, China). Stained sections were imaged using a PANNORAMIC MIDI II (3D Histech, Hungary) and photos were analyzed by SlideViewer and Visiopharm. The following antibodies were employed here: DAPI (#D9542, Sigma), CD206 (#ab64693, Abcam), CD31 (#77699, CST), and F4/80 (#70076, CST).

2.16. Treatment plan design and conduct in phase I clinical trial

The dose-escalation part of the multicenter, open-label phase I study (ChiCTR2100045380) was conducted in Beijing Tiantan Hospital. Patients underwent 5, 15, and 30 mg SYHA1813 once-daily treatment, respectively, for a period of 21 days as a cycle until PD, unacceptable toxicity, or another discontinuation criterion was met. This study is being conducted in compliance with the Declaration of Helsinki, the International Council for Harmonisation Guidelines for Clinical Practice, and applicable local regulatory requirements. The protocol has been approved by the Ethics Committee of Beijing Tiantan Hospital (approval number: YW2020-053-02). All patients provided written informed consent before participation. The study enrolled patients aged $\geq$18 years with histologically or cytologically confirmed, recurrent, or advanced solid tumors, including but not limited to high-grade gliomas. Additional inclusion criteria included measurable disease with Response Assessment in Neuro-Oncology (RANO), Karnofsky $\geq$ 60; and adequate renal, liver, and hematologic function.

2.17. Ethics statement

The phase I clinical study was conducted under clinical protocols approved by the Ethics Committee of Beijing Tiantan Hospital Affiliated with Capital Medical University (approval number: YW2020-053-02). We obtained written informed consent from all participants per the principles established by the Helsinki Declaration. All animal experiments were carried out by the Guide for the Care and Use of Laboratory Animals and approved by the Shanghai Institute of Materia Medica Animal Care and Use Committee.

2.18. Statistical analysis

All data were presented as mean ± standard deviation (SD) or mean ± standard error of mean (SEM). Two samples were analyzed with an unpaired two-tailed student *t*-test for equal variance. Survival data were analyzed by Kaplan−Meier survival curves and comparisons were performed by log-rank test.

3. Results

3.1. SYHA1813 is a potent and selective inhibitor of VEGFRs and CSF1R

We rationally designed and synthesized a series of inhibitors of VEGFR and CSF1R based on our previously developed indazolylnaphthamide compounds[25], among which SYHA1813 stood out as a distinct one (Fig. 1A). It exhibited high potency against VEGFR-1, -2, and -3, with IC_{50} values of 2.8, 0.3, and 4.3 nmol/L, respectively (Fig. 1B; Supporting Information Table S1). Compared to Axitinib, an FDA-approved VEGFR inhibitor, SYHA1813 exhibited similar inhibitory activity against VEGFR-2 and a slightly weaker effect against VEGFR-1 and -3. Meanwhile, SYHA1813 also effectively inhibited CSF1R kinase activity, with IC_{50} of 19.3 nmol/L (Fig. 1B; Table S1), which was comparable to that of PLX3397, an approved CSF1R inhibitor for the treatment of giant cell tumor of the tendon sheath, a benign soft tissue tumor. Meanwhile, the results of SPR demonstrated a robust binding signal between SYHA1813 and VEGFR-2 or CSF1R (Supporting Information Fig. S1). We then profiled SYHA1813 against a panel of 328 kinases to identify other potential targets of this compound and the result showed that most of the kinases showed less than 80% inhibition relative to the control at 0.1 μmol/L SYHA1813 (Fig. 1C). The kinases that exhibited more significant than 50% inhibition were then selected for further measurement the inhibitory activities, and SYHA1813 showed weak inhibition on these kinases, with IC_{50} values more than 100-fold higher than that of VEGFR-2 (Supporting Information Table S2). These results established that SYHA1813 was a potent and selective inhibitor of CSF1R and VEGFR.

To confirm the binding mode responsible for the observed potency, a docking study was conducted between SYHA1813 and the kinase domain of VEGFR-2 or CSF1R[26,27]. SYHA1813 is bound to the ATP binding site of VEGFR-2 (Fig. 1D) or CSF1R (Fig. 1E) in a "DFG-out" conformation. The 3-aminoindazole scaffold mimicked the adenine of ATP, forming three canonical hydrogen bonds with the hinge region of both targets. The naphthamide portion extended into the hydrophobic pocket of the protein and formed a hydrogen bond between the amide NH of SYHA1813 and the side chain carbonyl of VEGFR-2 Glu 885 or CSF1R Glu 633, significantly enhancing the inhibitor-kinase binding affinity.

3.2. SYHA1813 influences macrophage cell viability and suppresses angiogenesis

The cellular activities of SYHA1813 against CSF1R were then examined in macrophages. SYHA1813 dose-dependently inhibited the CSF1-stimulated cell viability of bone marrow-derived macrophages (BMDMs) (Fig. 2A). Western blot results confirmed the phosphorylation of CSF1R, as well as the activation of downstream AKT in BMDM cells (Fig. 2B) and murine peritoneal macrophages Raw264.7 cells (Supporting Information Fig. S2A) were dramatically blocked by SYHA1813, respectively. We also addressed whether glioma cells supplied CSF1 support CSF1R activation in macrophages and whether it could be blocked in the presence of SYHA1813. Mouse glioma DBT cells were proved to express a high level of CSF1 (Fig. S2B), and the tumor-conditioned medium (TCM) of DBT cells effectively activated CSF1R in Raw264.7 macrophages (Fig. S2C). As expected, SYHA1813 treatment efficiently blocked the CSF1R activation and downstream signaling transduction induced by the TCM (Fig. S2C). The results indicate that SYHA1813-mediated blockade of CSF1R effectively suppresses the activation of CSF1R signaling and impedes macrophage cell viability. We then analyzed how CSF1R blockade by SYHA1813 might impact the *in vitro* differentiation of macrophages. Cytokines CSF1, IL4, and IL13 were added to the BMDM cells to stimulate the macrophages, and flow cytometry was used to detect and analyze the expression of M2 markers CD206 and ARG1. As shown in

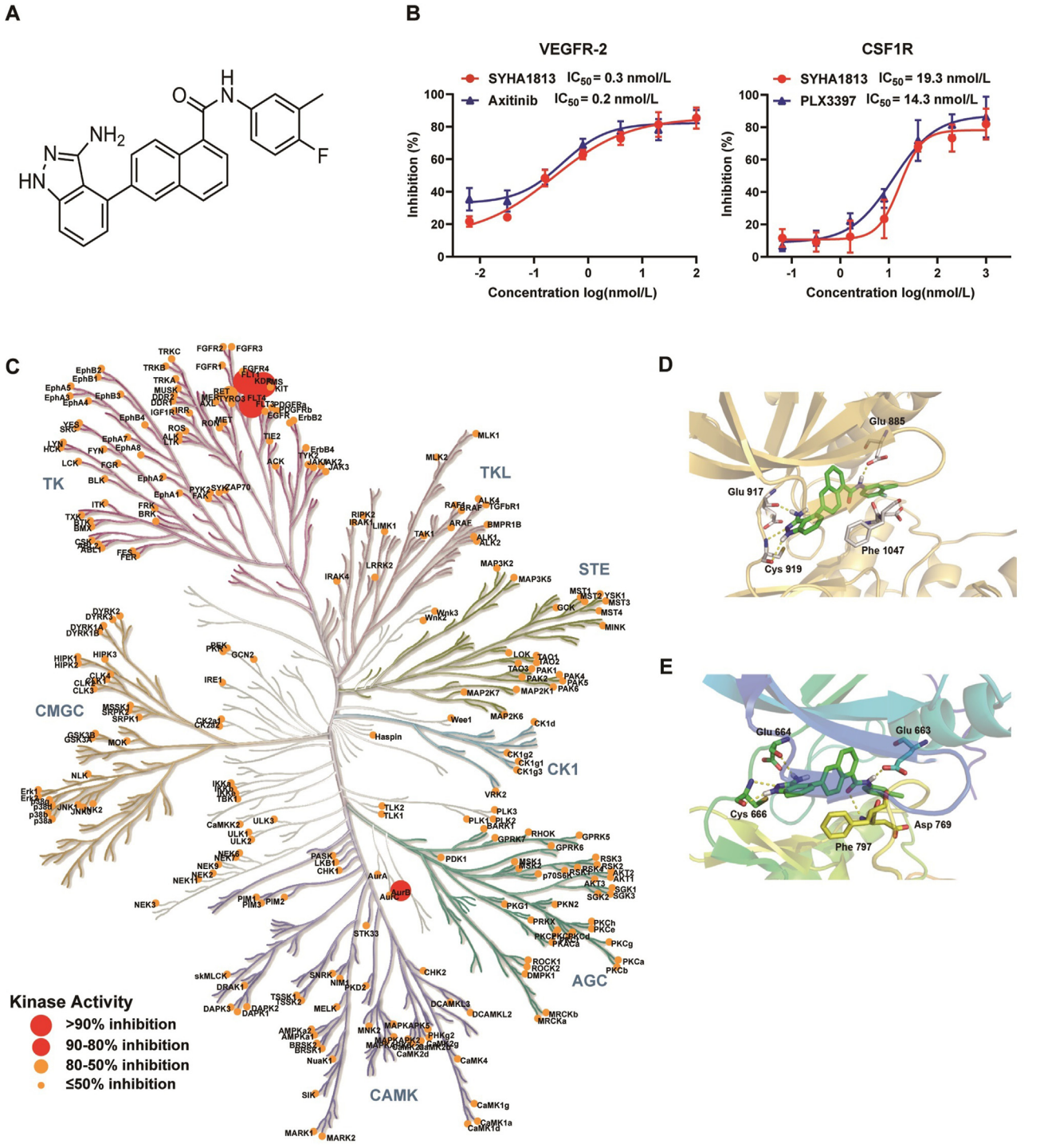

Figure 1 Structure and kinase inhibitory profile of SYHA1813. (A) The chemical structure of SYHA1813. (B) SYHA1813 dose-dependently inhibited VEGFR-2 and CSF1R kinase activity. IC_{50} values are shown as mean ± SD from three independent experiments. The *x*-axis is displayed on a logarithmic scale. (C) The kinase profiling data of SYHA1813. Activities of 328 kinases under SYHA1813 at the condition of 0.1 μmol/L were examined and the results were plotted in a representation of the human kinome using KinMap, with slight modifications. Illustration reproduced courtesy of Cell Signaling Technology, Inc (www.cellsignal.com). The size of the circles indicates the inhibition rate of SYHA1813 against the kinase. (D, E) Proposed binding model of SYHA1813 to VEGFR-2 or CSF1R kinase domain. SYHA1813 binds to VEGFR-2 (D) or CSF1R (E) in a "DFG-out" confirmation, forming three H-bonds between the 3-aminoindazole template and ATP binding domain, as well as an H-bond between amide NH and allosteric area of the proteins.

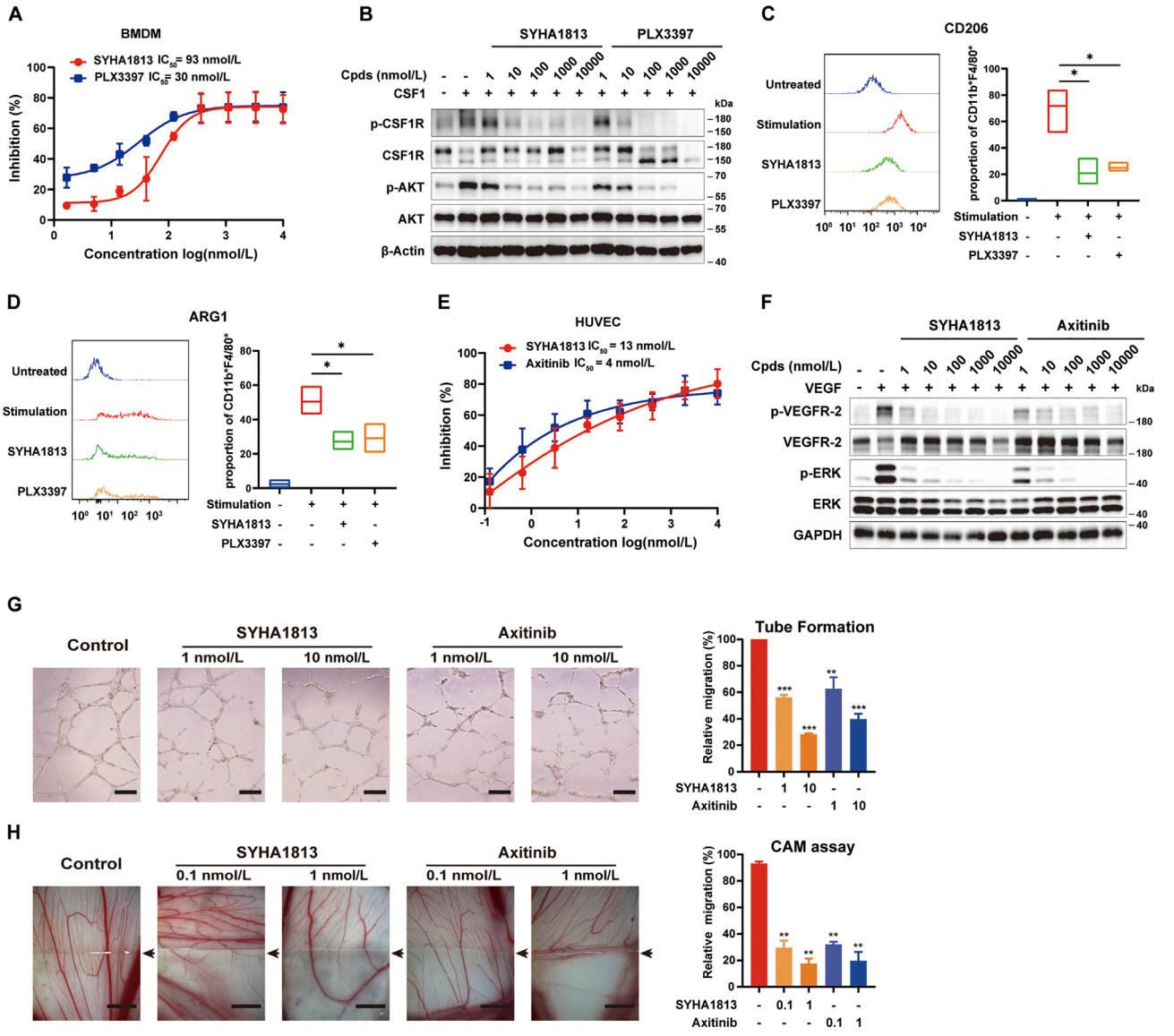

Figure 2 SYHA1813 influences the cell viability and differentiation of BMDMs and suppresses angiogenesis. (A) SYHA1813 influenced the CSF1-mediated cell viability of BMDMs. PLX3397 was used as a positive control. IC_{50} values were shown as mean ± SD from three independent experiments. (B) The phosphorylation of CSF1R and AKT in BMDMs was effectively inhibited upon SYHA1813 or PLX3397 treatment. (C, D) The expression of CD206 (C) and ARG1 (D) in BMDMs was decreased upon SYHA1813 treatment. Cells were stimulated with CSF1 (100 ng/mL), IL4 (10 ng/mL), and IL13 (10 ng/mL) and then treated with or without compounds. Flow cytometry was performed to detect the expression of CD206 and ARG1. The data were statistically analyzed by *t*-test from the results of three independent experiments (*$P < 0.05$, **$P < 0.01$). (E) SYHA1813 inhibited the VEGF-mediated proliferation of HUVEC. IC_{50} values were shown as mean ± SD from three independent experiments. (F) Western blot analysis of HUVEC treated with or without compounds. SYHA1813 effectively inhibited the VEGF-induced phosphorylation of VEGFR-2 and the activation of downstream molecule ERK. Axitinib was used as a positive control. (G) SYHA1813 inhibited the tube formation of HUVECs (scale bars: 0.2 mm). (H) SYHA1813 inhibited the angiogenesis in the CAM model. Cover glass saturated with or without compounds was placed on the lower side of each field. Arrows indicate the edge line of the cover glass (scale bars: 2 mm).

Fig. 2C and D, cytokines stimulation increased the expression of M2 markers compared to the control group. In contrast, SYHA1813 or PLX3397 treatment group demonstrated a significant decrease in the expression, indicating CSF1R blockade by the inhibitors effectively suppressed the differentiation of BMDM cells into M2 phenotype.

As VEGFR signaling is critical in the process of angiogenesis, we further detected the antiangiogenic activity of SYHA1813. The potency of SYHA1813 against endothelial cell viability was assessed using HUVECs. SYHA1813 inhibited the VEGF-stimulated cell viability of HUVEC cells in a dose-dependent manner, with IC_{50} value at 13 nmol/L (Fig. 2E). It also markedly inhibited VEGF-induced activation of VEGFR-2 in HUVECs, as well as the phosphorylation of ERK, one of the critical molecules downstream of VEGFR (Fig. 2F), suggesting the VEGFR-2 inhibition largely accounted for the growth inhibition of HUVECs caused by SYHA1813. *In vitro*, angiogenic experiments demonstrated that SYHA1813 considerably blocked the tube formation of HUVECs in a concentration-dependent manner (Fig. 2G). In an *in vivo* chorioallantoic membrane

(CAM) assay, which recapitulates the critical steps in the angiogenesis process, neovascularization in chick embryos was also significantly inhibited after SYHA1813 treatment (Fig. 2H). These data supported that SYHA1813 possessed potent anti-angiogenic activities *in vitro* and *in vivo*.

3.3. SYHA1813 blocks tumor growth in GBM xenograft models including TMZ insensitive tumor by inhibiting VEGFR and CSF1R

We evaluated the *in vivo* efficacy of SYHA1813 against GBM in mouse models. Nude mice bearing established U251 GBM xenograft tumors were treated with SYHA1813 twice daily. SYHA1813 treatment substantially inhibited subcutaneous tumor growth compared to vehicle-treated mice (Fig. 3A). Treatment of 5 and 10 mg/kg SYHA1813 considerably reduced 67.7% and 81.0% tumor volume, respectively, which was more potent than Axitinib at the dosage of 40 mg/kg. The Western blot results showed that the phosphorylation of CSF1R and VEGFR-2 in the U251 tumor tissue was markedly inhibited upon SYHA1813 treatment (Supporting Information Fig. S3). Following the same protocol, we verified the inhibition of tumor growth by SYHA1813 using another human GBM xenograft tumor, U87MG, and similar observations were recapitulated (Fig. 3B). Moreover, we also established the D283 medulloblastoma xenograft model, which was reported previously that was insensitive to TMZ treatment, mainly because of the activation of tumor DNA repair systems that removes TMZ-induced DNA adducts and restores genomic integrity. Compared to TMZ-sensitive U87MG xenograft models, D283 xenograft tumors were dramatically insensitive to TMZ treatment, whereas SYHA1813 treatment effectively inhibited tumor growth in a dose-dependent manner (Fig. 3C; Supporting Information Fig. S4). The body weight of the animals in each model was not significantly changed upon SYHA1813 treatment (Fig. 3D). These results collectively indicated demonstrated that SYHA1813 has robust anti-tumor efficacy at well-tolerated doses in xenograft models of GBM, including TMZ insensitive tumor.

We then further examined the markers of macrophage and angiogenesis in tumors. SYHA1813 treatment dramatically reduced the expression of the angiogenic markers, CD31 and CD105, in U251 tumor tissues compared with control (Fig. 3E). It also significantly inhibited the expression of the M2 phenotype marker of macrophage CD206 in tumor (Fig. 3E). Similar results were also observed in U87MG xenograft tumors, as demonstrated by the decreased expression of CD31, CD105, CD206, and CD163 in SYHA1813-treated tumors (Supporting Information Fig. S5). Ki67 proliferation marker was also significantly decreased upon SYHA1813 treatment (Fig. S5). As expected, Axitinib, an inhibitor targeting VEGFR but not CSF1R, effectively suppressed the expression of angiogenic markers CD31 and CD105, while causing no significant changes in M2 phenotype macrophage markers (Fig. 3E; Fig. S5). These data demonstrated that SYHA1813 exhibited anti-tumor activities through re-educating macrophages and suppressing angiogenesis in tumors.

3.4. SYHA1813 effectively crosses the BBB and prolongs the survival time of mice with intracranial GBM tumors

Pharmacokinetic studies were carried out on CD-1 mice. SYHA1813 was given at a dosage of 10 mg/kg by oral gavage and showed favorable pharmacokinetics (Supporting Information Table S3). We found that the maximum concentration (C_{max}) of SYHA1813 in brain tissue (1214 ng/g) was close to that in plasma (1417 ng/mL), and the amount of exposure in brain tissue (5008 h ng/g) was even slightly higher than in plasma (4545 h ng/mL) (Fig. 4A; Table S3). These data indicated that SYHA1813 could effectively cross the BBB, which is a significant advantage over other VEGFR inhibitors that have been reported.

We were then particularly interested in whether orally-administered SYHA1813 could efficiently suppress the growth of intracranial GBM tumors. To this end, we established luciferase-modified U87MG xenografts in the brains of mice (Fig. 4B). The mice bearing intracranial tumor were established for 7 days before treatment started. On Day 8, SYHA1813 (40, 20 mg/kg) was administered orally twice daily with the endpoint measuring survival. Bioluminescence monitoring showed sustained anti-tumor activity throughout SYHA1813 treatment (Fig. 4C). The death of the control group began on Day 31, and the last death of this group was on Day 52, with the median survival time at 41 days (Fig. 4D). Not surprisingly, the survival of mice in each SYHA1813 treatment group was extended to varying degrees. The death of mice in the 40 mg/kg experimental treatment group was not seen until Day 43, and the death of the last mouse was on Day 75. The median survival time of 20 and 40 mg/kg SYHA1813 groups were 54 and 58.5 days, respectively, which were significantly longer than that of the control group (Fig. 4D). Meanwhile, the median survival of Axitinib treatment group was 41 days, with no improvement in survival compared to the control group (Fig. 4D). Moreover, we also investigated the antitumor efficacy of SYHA1813 on a mouse glioma GL261-luc model in immunocompetent mice and analyzed the effect on tumor immune microenvironment. The data of IVIS spectroscopy indicated that SYHA1813 treatment resulted in a strong growth inhibition of intracranial tumor (Supporting Information Fig. S6A and S6B) and a prolonged median survival time (Fig. 4E). The cytometry by time-of-flight mass spectrometry (CyTOF) analysis demonstrated a significant reduction in F4/80-positive macrophages following SYHA1813 treatment, accompanied by a notable decrease in $PDL1^+$ macrophage and regulatory T cells (Tregs) within the treated cohort (Fig. 4F). Additionally, immunofluorescence analysis was employed to further investigate the expression of macrophage and angiogenesis markers in tumors. Treatment with SYHA1813 significantly decreased the levels of CD31 (Fig. 4G) and F4/80 (Fig. 4H) in tumor tissues compared to the control group. Although a reduction in CD206 alterations was observed, there was no statistically significant difference (Fig. S6C). These data demonstrated that SYHA1813 exhibited potent intracranial anti-tumor activities through alleviating macrophage-mediated immunosuppression and suppressing angiogenesis in tumors.

3.5. SYHA1813 modulates the tumor immune microenvironment and synergizes anti-PD-1 immunotherapy in glioma

As both TAM and angiogenesis contribute to immunosuppressive TME, we assumed that SYHA1813 could modulate TME and might enhance the antitumor effect of PD-1-targeted therapy. We thus first evaluated the efficacy of SYHA1813 against the DBT mouse glioma model in immunocompetent animals. As expected, tumor growth of DBT glioma and tumor weight were suppressed in mice treated with 10 mg/kg SYHA1813 twice daily (Fig. 5A).

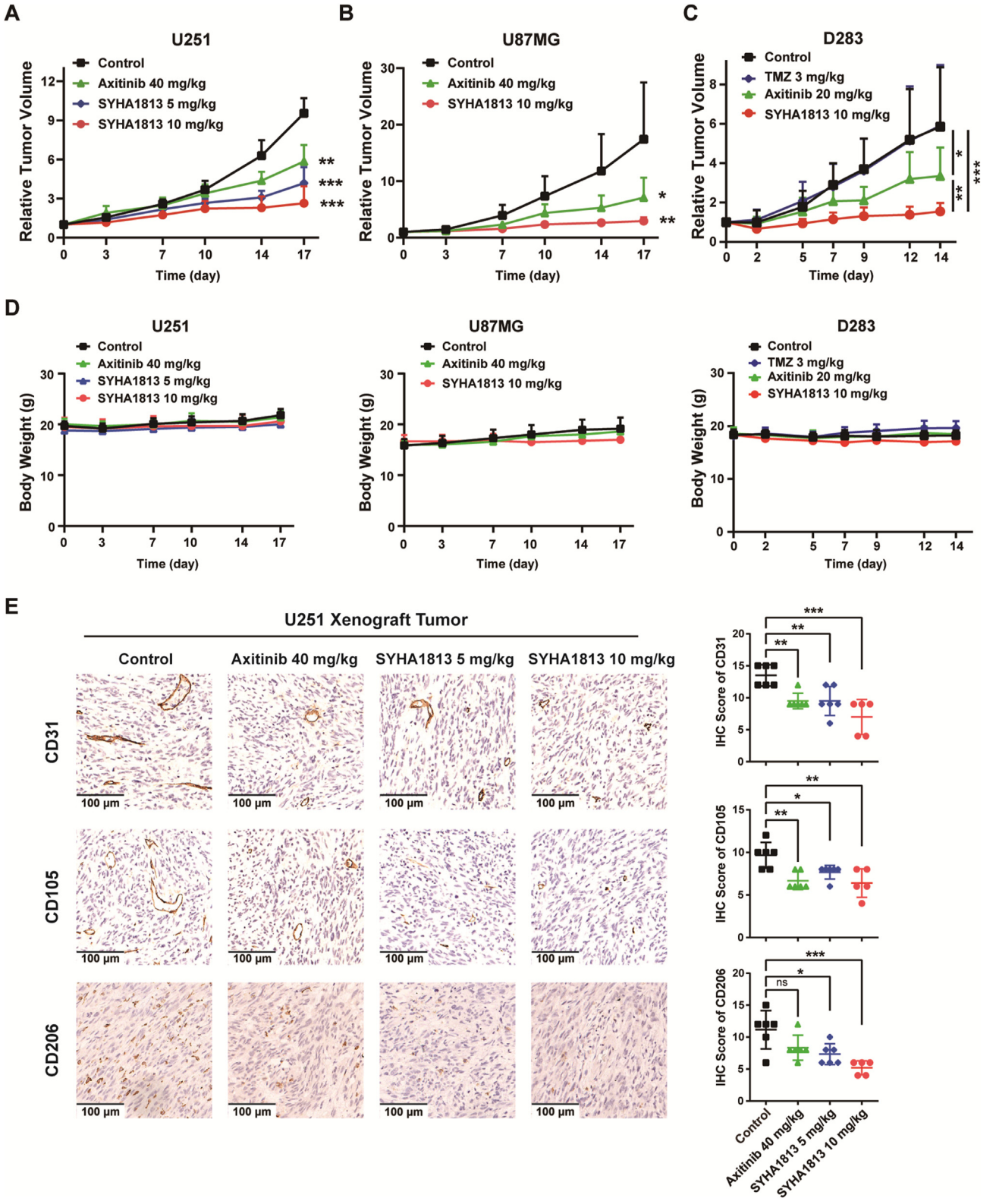

Figure 3 SYHA1813 exhibits anti-GBM activity in immunodeficiency mouse models. (A, B) SYHA1813 inhibited the tumor growth of U251 (A) and U87MG (B) xenograft tumors. The tumor volumes were monitored twice a week and expressed as the mean ± SD, $n = 6$. (C) Antitumor activity of SYHA1813 in the TMZ-insensitive D283 xenograft model. Data are exhibited as mean ± SD, $n = 9$. (D) The body weights of mice in U251, U87MG, and D283 xenograft models were recorded. Data are exhibited as mean ± SD. (E) The expression of M2 phenotype macrophage markers (CD206) and angiogenesis markers (CD31, CD105) in the U251 tumor tissue were examined using IHC. Representative images were displayed. Brown staining indicates positivity (scale bars: 100 μm; $n = 5$ or 6). The IHC scores were quantified by the multiplicative quick score method. Data were analyzed using *t*-test, $^{*}P < 0.05$, $^{**}P < 0.01$, $^{***}P < 0.001$.

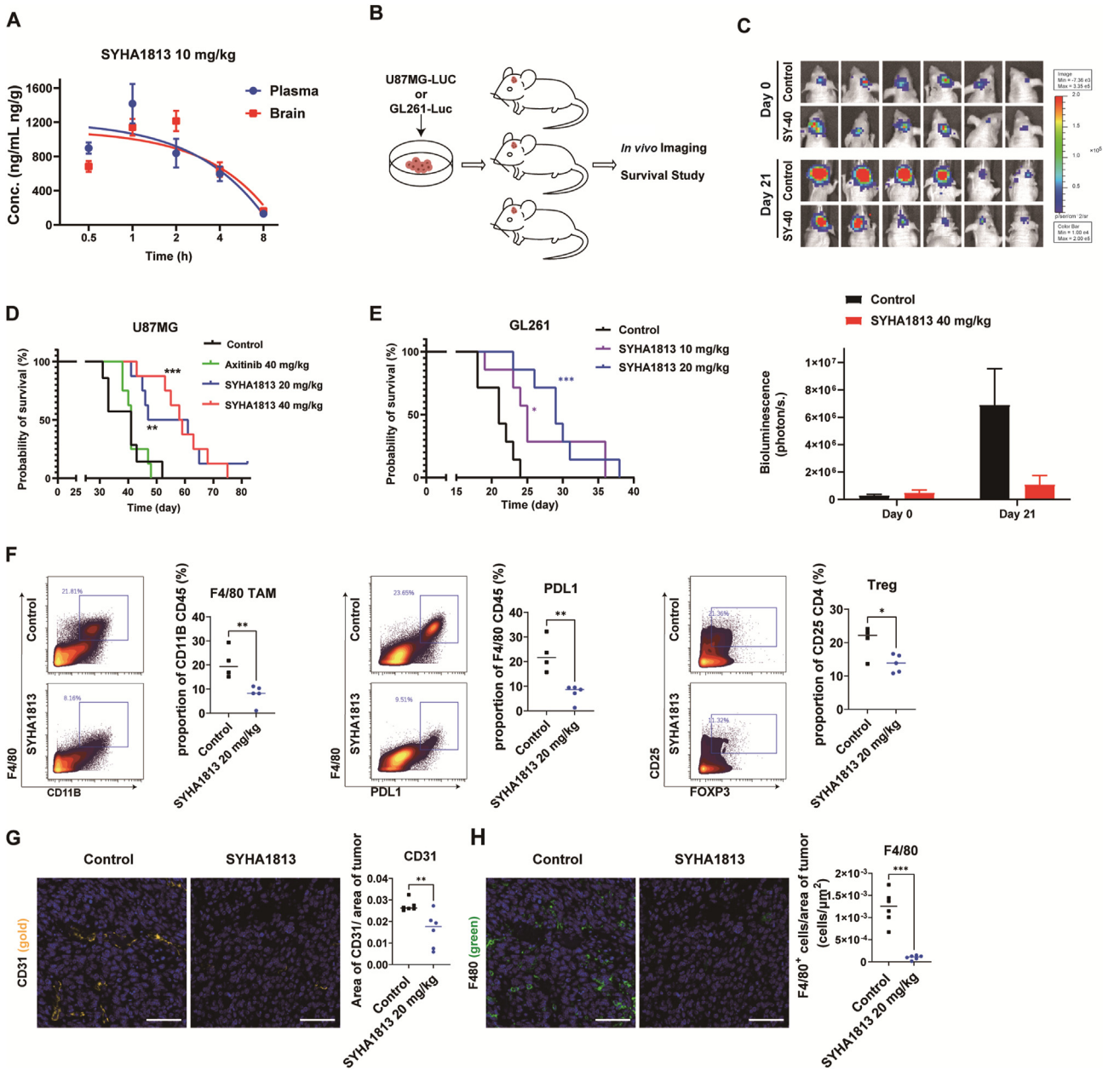

Figure 4 SYHA1813 effectively crosses the BBB and prolongs the survival of mice with glioma tumor *in situ*. (A) The distribution of SYHA1813 in the brain and plasma of CD-1 mice after *p.o.* administration of SYHA1813 at 10 mg/kg. Data are presented as mean ± SEM, $n = 5$. (B) Diagram of intracranial tumor model in nude mice. (C) The fluorescence intensities of mice treated with SYHA1813 at 40 mg/kg (SY-40) or vehicle control were recorded on Day 21. Data are presented as mean ± SEM, $n = 7$. (D) SYHA1813 significantly prolonged the median survival time of mice with intracranial glioma tumor U87MG. Data were analyzed using Log-rank (Mantel−Cox) test, $^{*}P < 0.05$, $^{**}P < 0.01$, $^{***}P < 0.001$, $n = 7$. (E) SYHA1813 significantly prolonged the median survival time of mice with intracranial mouse glioma tumor GL261-Luc. Data were analyzed using Log-rank (Mantel−Cox) test, $^{*}P < 0.05$, $^{**}P < 0.01$, $^{***}P < 0.001$, $n = 7$. (F) The presence of $F4/80^{+}$ macrophages, $PDL1^{+}F4/80^{+}$ macrophages, and Tregs ($CD4^{+}CD25^{+}FOXP3^{+}$) in GL261-luc tumor tissue was analyzed using CyTOF in both control and treatment groups. Data were analyzed using *t*-test, $^{*}P < 0.05$, $^{**}P < 0.01$, $^{***}P < 0.001$, $n = 5$. (G, H) The expression of angiogenesis marker (CD31, gold) and macrophages marker (F4/80, green) in the brain tumor tissue of GL261-Luc were examined using immunofluorescence. Representative images are displayed (scale bars: 50 μm; $n = 6$).

Immunohistochemistry analysis showed that the expression of M2 phenotype macrophage marker CD163 was significantly decreased in SYHA1813 treatment group than the vehicle control group (Fig. 5B), which was consistent with the results discovered in U87MG and U251 xenograft models. Of particular note, the $CD8^{+}$ T cells in tumor tissue were dramatically increased upon SYHA1813 treatment (Fig. 5B), indicating that it could rescue T cell exhaustion in glioma.

Based on these encouraging observations, we further investigated whether the combination of SYHA1813 with PD-1-targeted

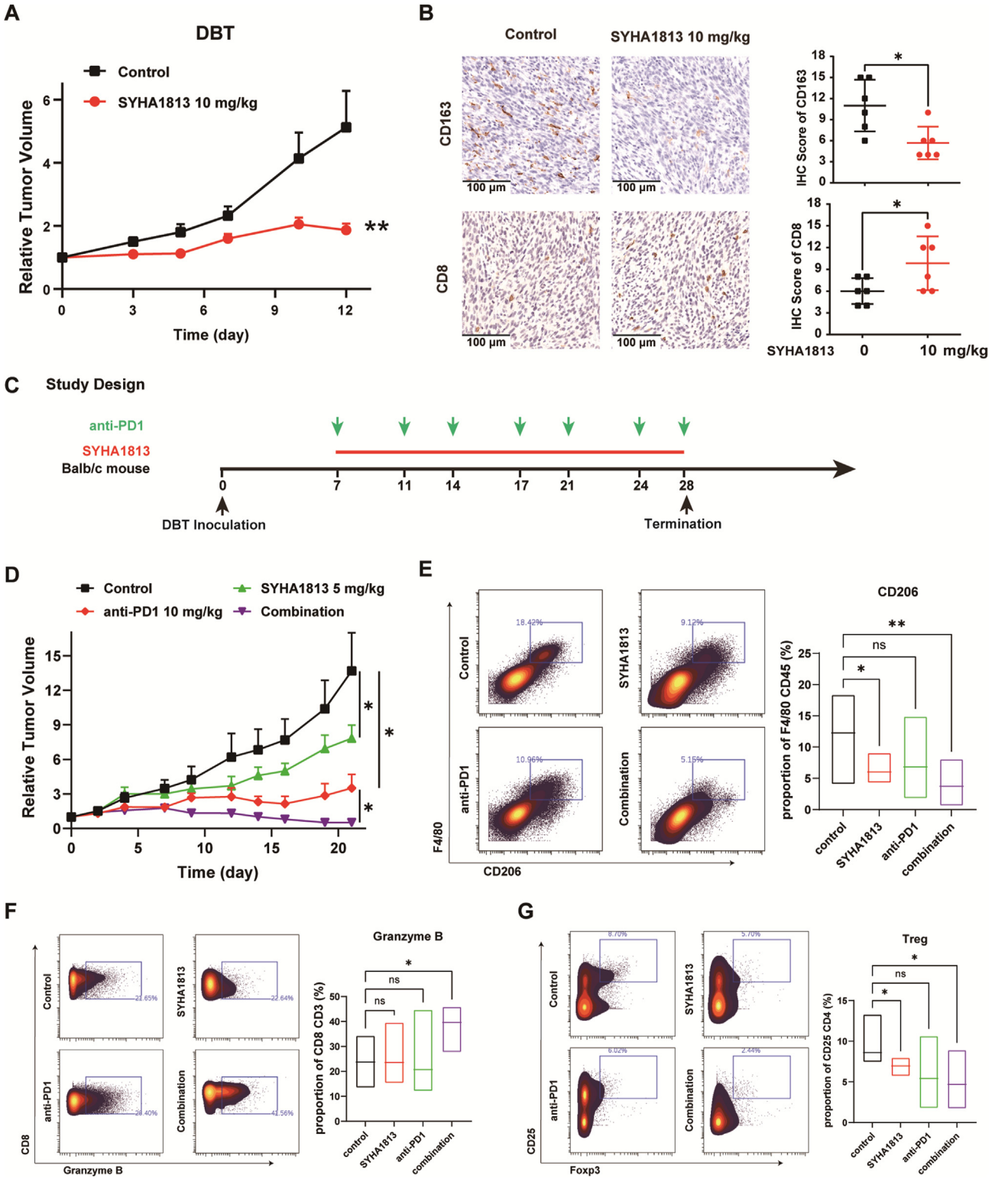

Figure 5 Combination of SYHA1813 and anti-PD-1 antibody produces synergistic effects against glioma in immunocompetent mouse allograft model. (A) SYHA1813 suppressed the *in vivo* DBT tumor growth. BALB/c mice bearing with established DBT tumors were orally administered with or without SYHA1813 (10 mg/kg, twice daily). The RTVs are expressed as the mean ± SEM. (B) The expression of CD163 and CD8 in the tumor tissue was examined using IHC. (C) Diagram of combination study of SYHA1813 with PD-1 antibody in DBT mouse model. (D) SYHA1813 enhanced the anti-tumor activity of the anti-PD-1 antibody. The RTVs are expressed as the mean ± SEM, $n = 6$. (E) The $CD206^{+}F4/80^{+}$ macrophage in tumor tissue in control or administrated groups was detected by CyTOF. Data were analyzed using *t*-test, $^{*}P < 0.05$, $^{**}P < 0.01$, $^{***}P < 0.001$. (F, G) The expression of Granzyme B (F) in $CD8^{+}$ T cell, Treg ($CD4^{+}CD25^{+}FOXP3^{+}$) (G) in the tumor tissue were also detected by CyTOF. Data were analyzed using a *t*-test, $^{**}P < 0.01$, $^{***}P < 0.001$, $n = 6$.

therapy could result in synergistic treatment effects in mouse glioma models (Fig. 5C). The results demonstrated that tumor growth was slightly inhibited by SYHA1813 alone ($P < 0.05$) and was moderately inhibited by anti-PD-1 antibody alone ($P < 0.05$) (Fig. 5D). In contrast, the growth was significantly suppressed in the combination therapy group, compared to control ($P < 0.01$), SYHA1813 alone group ($P < 0.01$) and anti-PD-1 monotherapy group ($P < 0.05$) (Fig. 5D), clearly indicating that the combination therapy produced synergistic antitumor efficacy. Moreover, the CyTOF results showed that the infiltration of TAM ($CD206^+$ $F4/80^+$ in $CD45^+$ cells) in tumor tissue was significantly inhibited, especially in the combined treatment group (Fig. 5E). The expression of iNOS in the combined treatment group was significantly increased, suggesting that the tumor-killing ability of macrophages were enhanced. The reduced expression of PDL1 indicated the alleviation of immunosuppression in tumor tissue (Supporting Information Fig. S7A and S7B). Meanwhile, combination treatment significantly upregulated the invasion of lethal Granzyme B^+ T cells, and down-regulated the Treg ($Fxop3^+$) and $PD1^+$ T cells, confirming the immunosuppression of T cells was primarily relieved (Fig. 5F and G, Fig. S7C). These results demonstrated that this combination therapy could reduce macrophage immunosuppression and enhance T cell cytotoxicity in TME.

3.6. *Proof-of-concept clinical activity*

SYHA1813 is being investigated in an ongoing first-in-human dose-escalation phase I clinical trial (ChiCTR2100045380) in patients with recurrent high-grade glioma, brain metastasis, and advanced solid cancers. All patients underwent surgical treatment and had received prior systemic therapy.

Here, we provided imaging data of the first three patients who underwent 5, 15, and 30 mg once-daily treatment, respectively, for a period of 21 days as a cycle (Fig. 6A and B). There were significant changes in both T1 postcontrast enhancement and T2-weighted or fluid-attenuated inversion recovery (FLAIR) abnormality before and after the treatment with SYHA1813 from brain magnetic resonance imaging (MRI) in these patients. The first recurrent patient (anaplastic oligodendrocytoma) participated in the SYHA1813 clinical trial after evaluation (Fig. 6A). Five milligrams of SYHA1813 were administered. After 4 cycles of treatment, T1 post-contrast enhancement demonstrated that lesions had a striking change in size. Response Assessment in Neuro-Oncology (RANO) was assessed as a stable disease. Our second subject was recurrent GBM (WHO IV) and was treated with SYHA1813 (15 mg/day). The patient treated with SYHA1813 experienced a drastic reduction in both contrast-enhancement on T1-weighted images and vasogenic edema on FLAIR images at the first follow-up time-point, and meanwhile, the clinical symptoms were significantly improved (Fig. 5A). The third patient participated in SYHA1813 clinical trial of 30 mg/day dose group. The patient had either a response on FLAIR or post-contrast T1-weighted images after one cycle of treatment, MRI showed one of the lesions disappeared, and the other lesion was significantly reduced, which achieved PR (Fig. 6C).

Collectively, our data demonstrated that SYHA1813 exerted potent anti-GBM activity *via* targeting CSF1R and VEGFR. It also showed promising anti-GBM efficacy in an ongoing clinical study, supporting further development for the treatment of GBM.

4. Discussion

GBM is the most common and aggressive adult primary brain tumor. Unfortunately, despite numerous efforts of researchers worldwide, no small-molecule targeted agents have been successfully used for GBM treatment[28]. Chemotherapy is one of the effective methods for the treatment of glioma. However, due to the unique structure of BBB, it is difficult or impossible for available chemotherapy drugs to pass through the BBB. TMZ is the first-line chemotherapy drug for glioma at present, but more than half of patients do not respond to TMZ and face the problem of high recurrence. In addition, TMZ has side effects such as bone marrow suppression, genotoxicity, and reproductive toxicity, which affect its long-term use. Malignant gliomas are characterized by a marked increase in angiogenesis, which is crucial for tumor growth and colonization in the brain[29]. Bevacizumab, a monoclonal antibody that inhibits angiogenesis by targeting VEGF-A, has been administered intravenously for the treatment of recurrent GBM[30]. However, as the antibody cannot penetrate the BBB, the efficacy of systemic treatment with bevacizumab is reduced significantly resulting in no improvement in the overall survival of GBM patients[31,32]. Therefore, current available therapies only minimally improve the prognosis of glioma patients, and new therapeutic agents are desperately needed.

A hallmark adaptation of GBM is the development of a profoundly immunosuppressive TME that cripples endogenous antitumor immune responses and limits the effectiveness of immunotherapies[28,33,34]. As one of the vital immune-suppressive components of the brain TME, macrophages were identified as a promising therapeutic target for GBM, and CSF1R inhibitors are particularly attractive as both the CSF1 expression level and the CSF1R positive macrophages have been shown to correlate with poor survival in glioma. TAMs have been identified to be a major source of angiogenic growth factors and play an important role in glioma resistance to anti-VEGF therapy[35,36]. Conversely, vascular enrichment may also be one of the critical reasons for GBM resistance to CSF1R inhibitor[21]. Therefore, targeting TAMs might complement antiangiogenic therapies and improve the effectiveness, while targeted angiogenesis can overcome CSF1R inhibitor resistance. All of these researches collectively highlight the potential importance and urgent need for identifying novel VEGFR/CSF1R dual inhibitors for GBM therapy. Here we described the identification and characterization of a novel and potent inhibitor of CSF1R and VEGFR, SYHA1813. It inhibited the phosphorylation of CSF1R in macrophages and modulated the macrophages into an antitumor phenotype. It also suppressed the activation of VEGFR in HUVECs and thus exhibited potent anti-angiogenetic effects.

Kinase profiling results showed that SYHA1813 also inhibited a few kinases other than VEGFR and CSF1R. Among the kinases with an inhibition rate greater than 50% at 100 nmol/L SYHA1813, c-Kit, and PDGFRα mutations, Aurora-B and RET have attracted our attention. We conducted an ELISA assay to examine the activity of SYHA1813 against wild-type and mutated forms of c-Kit and PDGFRα kinases. As shown in Supporting Information Table S4, SYHA1813 displayed moderate inhibition towards c-Kit and c-Kit (D816H) mutant, with IC_{50} values of 162.5 and 134.0 nmol/L, respectively, which is much weaker than that of SYHA1813 against VEGFR-2 (IC_{50} = 0.3 nmol/L). It also exhibited moderate inhibition against PDGFRα and PDGFRα (D842V) mutant, while potent inhibition against PDGFRα (V561D) was observed

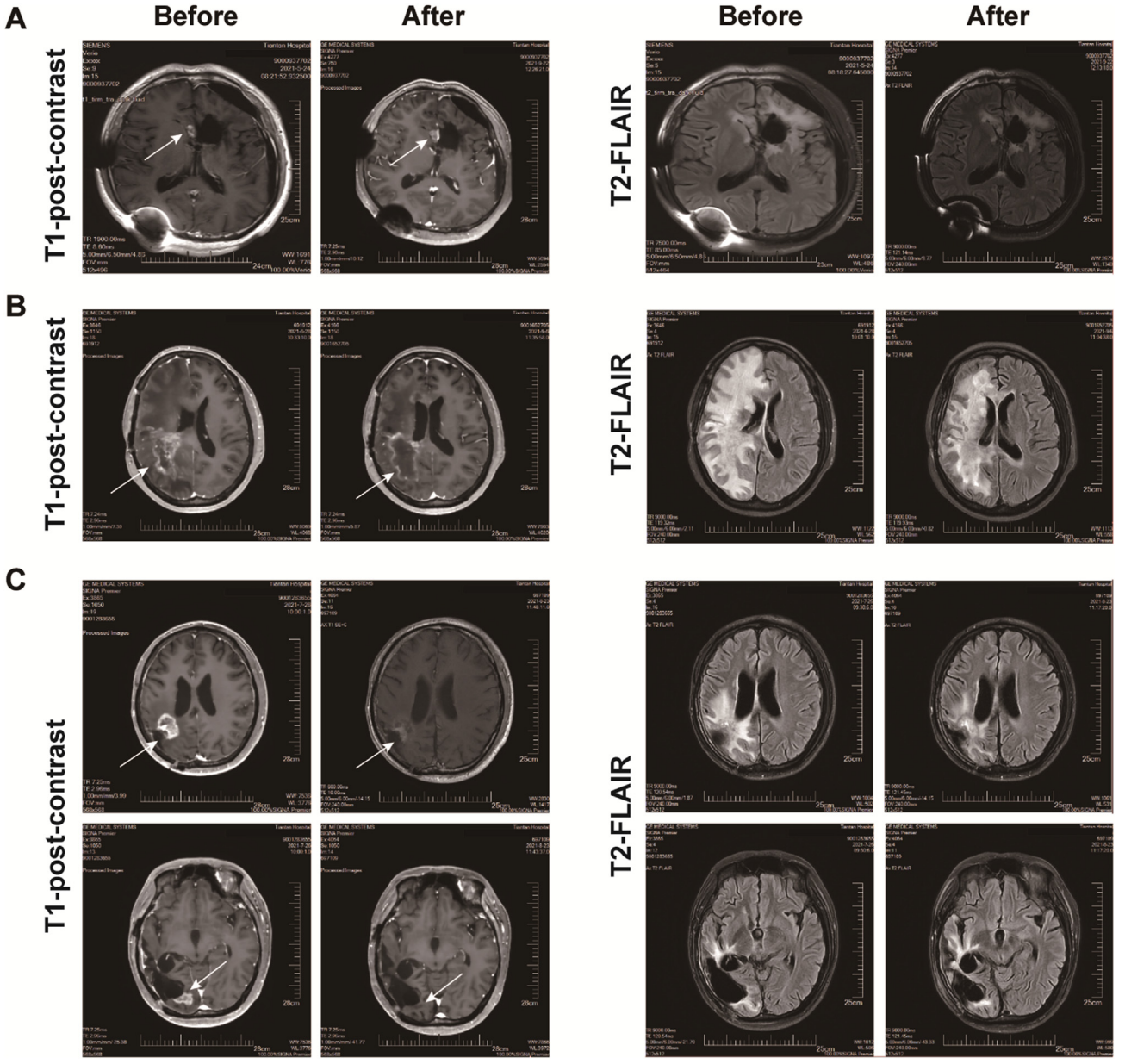

Figure 6 Response to SYHA1813 in the first three patients. (A) Pretreatment and 16-week scans of a patient with anaplastic oligodendrocytoma (WHO grade III) indicated the original lesions did not recur. The patient continues the study. (B) Baseline and 8-week (Cycle 2) scans of a patient with GBM (WHO IV) demonstrated the edema area volumes after treatment reduced apparently. (C) Baseline and 4-week (Cycle 1) scans of a patient with GBM (WHO IV). One of the lesions (above) at the edge of the operation area disappeared and the other lesion (below) was significantly reduced.

(IC_{50} = 2.4 nmol/L). As PDGFRα (V561D) mutation has been reported as one of the most prevalent mutations driving gastrointestinal stromal tumors (GISTs), further investigation of the therapeutic potential of SYHA1813 for PDGFRα V561D-mutated GIST is recommended for future studies. Cellular-level studies have shown that SYHA1813 has no apparent cytotoxicity to cells with high expression of Aurora-B (data not shown). Moreover, the phosphorylation of RET in tumor tissue was rarely inhibited upon SYHA1813 treatment (data not shown). Although many VEGFR inhibitors also possess inhibitory activity against CSF1R, almost all of them show inhibition against other kinases, such as FGFRs, c-KIT, PDGFRs, FLT3, or JAK, which results in uncontrollable toxicity and side effects in clinical studies[37]. Therefore, to our best knowledge, SYHA1813 is the first highly selective CSF1R/VEGFR inhibitor in clinical development.

Quantitative studies in mice brains with SYHA1813 treatment showed a pretty high brain concentration of SYHA1813, almost at the same level as in the blood, suggesting the excellent ability of SYHA1813 to penetrate the BBB. This result indicated an advantage of SYHA1813 over other VEGFR inhibitors or bevacizumab that have been reported and shed light on the potential value of SYHA1813 for clinical development in GBM treatment. Data from animal studies demonstrated SYHA1813 exhibited potent antitumor activities against glioma both in orthotropic (intracranial xenografts) and heterotopic xenograft mouse models through

modulating tumor immune microenvironment and inhibiting the angiogenesis of tumor. Of particular note, SYHA1813 also showed significant antitumor activity against TMZ-insensitive tumor models, suggesting a potential value of this compound for further clinical development in TMZ-insensitive and resistant tumors. In addition, SYHA1813 exhibits negligible inhibition against glioma cell lines, with IC_{50} values greater than 20 μmol/L. These data suggest that SYHA1813 may not exert a direct inhibitory effect on glioma cells either *in vitro* (Supporting Information Table S5).

Immune checkpoint inhibition with monoclonal antibodies targeting PD-1 protein or its ligand, PD-L1, has shown promise in preclinical studies for the treatment of GBM[38,39]. However, monotherapy of anti-PD-1 antibody has only demonstrated limited benefit in GBM, and thus, many clinical trials are ongoing to assess the combination therapy of ICBs with other therapies to enhance the therapeutic effects of anti-PD-1 treatment[40−42]. Accumulating evidence demonstrated that TAM and other myeloid cells contribute to an immunosuppressive TME, and CSF1R blockade has been shown to reduce T-cell-suppressive TAM infiltrates[43,44]. Meanwhile, the VEGF pathway plays a central role in suppressing the tumor-directed immune response and promoting angiogenesis[45]. Modulating this suppressive state in the TME through angiogenesis inhibition is also considered an attractive partnering strategy for ICBs[46,47]. Therefore, inhibitors targeting CSF1R or VEGFR represent a promising combination partner for T-cell-enhancing immunotherapies. Our study confirmed that SYHA1813, as a novel VEGFR/CSF1R inhibitor, effectively reduced T-cell-suppressive TAM infiltration, increased cytotoxicity of $CD8^+$ T cells in tumor, and thus produced a synergistic effect with anti-PD-1 therapy in the animal model, providing the preclinical rationale for the combination of SYHA1813 with PD-1 blockade to restore antitumor immune responses and inhibit GBM growth.

We further examined the antitumor activities of SYHA1813 in the phase I clinical trial. Intriguingly, the first three patients enrolled in SYHA1813 clinical trial all showed a good response, with two having a stable disease and one with partial remission, convincing that SYHA1813 is a very promising anti-GBM agent. Therefore, the findings in this work provide strong support for further clinical development of SYHA1813 in treating GBM patients. It will also be interesting to examine combination therapies involving SYHA1813 with chemotherapy, radiotherapy, immune checkpoint therapy, or inhibitors targeting activated gene products in other GBM core pathways. Determination of the full range of applications of this VEGFR/CSF1R dual inhibitor will hopefully lead to improved treatment for this devastating cancer.

5. Conclusions

This research work developed a potent and selective small molecular SYHA1813 targeting VEGFR and CSF1R, which can efficiently cross the BBB and exhibit a potent anti-tumor effect both in subcutaneous transplant and intracranial GBM model. In immune-competent mice, treatment with SYHA1813 alleviates macrophage-mediated immunosuppression and produced synergistic antitumor efficacy in combination with an immune-checkpoint inhibitor. As a clinical proof of concept, SYHA1813 achieved confirmed responses in patients with GBM in an ongoing first-in-human phase I trial. The research findings in this work provide strong support and new insight into drug discovery and further, provide a novel theoretical basis for the clinical development of SYHA1813 in treating GBM patients in the future.

Acknowledgments

This research was supported by grants from the Natural Science Foundation of China for Innovation Research Group (81821005), the National Natural Science Foundation of China (82273948 and 81573271), the "Personalized Medicines, Molecular Signature-based Drug Discovery and Development", Strategic Priority Research Program of the Chinese Academy of Sciences (XDA12020203 and XDA12020228, China), the National Science & Technology Major Project "Key New Drug Creation and Manufacturing Program", China (2018ZX09711002-011-016), and the Youth Innovation Promotion Association of CAS (2018324, China).

Author contributions

Jian Ding, Hua Xie, Wenhu Duan, Wenbin Li and Meiyu Geng designed and supervised this work. Hua Xie, Yingqiang Liu, Zhengsheng Zhan, Zhuang Kang, Shenglan Li, and Yi Chen finished the original draft writing. Yingqiang Liu, Zhengsheng Zhan, Zhuang Kang, Shenglan Li, Mengyuan Li, Yongcong Lv, Fang Feng, Yan Li, Tao Zhang, Linjiang Tong, Mengge Zhang, Shanyan Yao, Yanyan Shen, Yiming Sun, Xinying Yang, Yi Su, Yi Chen and Yaping Xue performed the experiments. Yingqiang Liu, Zhengsheng Zhan, Zhuang Kang, Shenglan Li, Mengyuan Li, Fang Feng, Yan Li, Tao Zhang, Peiran Song, Linjiang Tong, Yongcong Lv, Yi Su, Xinying Yang and Yi Chen provided the technologies and the methods. Yingqiang Liu, Zhengsheng Zhan, Shenglan Li, Fang Feng, Yan Li, Linjiang Tong, Meiyu Geng, Yi Chen, Yi Su, Hanyu Yang and Caixia Wang performed the data analysis. Hua Xie, Yingqiang Liu, Hanyu Yang, Wenhu Duan, Wenbin Li and Jian Ding reviewed the paper.

Conflicts of interest

The authors declare no potential conflicts of interest.

Appendix A. Supporting information

Supporting data to this article can be found online at https://doi.org/10.1016/j.apsb.2023.09.009.

References

1. Wolf KJ, Chen J, Coombes J, Aghi MK, Kumar S. Dissecting and rebuilding the glioblastoma microenvironment with engineered materials. *Nat Rev Mater* 2019;**4**:651−68.
2. Aldape K, Brindle KM, Chesler L, Chopra R, Gajjar A, Gilbert MR, et al. Challenges to curing primary brain tumours. *Nat Rev Clin Oncol* 2019;**16**:509−20.
3. Janjua TI, Rewatkar P, Ahmed-Cox A, Saeed I, Mansfeld FM, Kulshreshtha R, et al. Frontiers in the treatment of glioblastoma: past, present and emerging. *Adv Drug Deliv Rev* 2021;**171**:108−38.
4. Klemm F, Maas RR, Bowman RL, Kornete M, Soukup K, Nassiri S, et al. Interrogation of the microenvironmental landscape in brain tumors reveals disease-specific alterations of immune cells. *Cell* 2020;**181**:1643−60.
5. Chuntova P, Chow F, Watchmaker PB, Galvez M, Heimberger AB, Newell EW, et al. Unique challenges for glioblastoma

immunotherapy-discussions across neuro-oncology and non-neuro-oncology experts in cancer immunology. Meeting Report from the 2019 SNO Immuno-Oncology Think Tank. *Neuro Oncol* 2021;**23**:356−75.
6. Van Overmeire E, Stijlemans B, Heymann F, Keirsse J, Morias Y, Elkrim Y, et al. M-CSF and GM-CSF receptor signaling differentially regulate monocyte maturation and macrophage polarization in the tumor microenvironment. *Cancer Res* 2016;**76**:35−42.
7. Pombo Antunes AR, Scheyltjens I, Lodi F, Messiaen J, Antoranz A, Duerinck J, et al. Single-cell profiling of myeloid cells in glioblastoma across species and disease stages reveals macrophage competition and specialization. *Nat Neurosci* 2021;**24**:595−610.
8. Pyonteck SM, Akkari L, Schuhmacher AJ, Bowman RL, Sevenich L, Quail DF, et al. CSF-1R inhibition alters macrophage polarization and blocks glioma progression. *Nat Med* 2013;**19**:1264−72.
9. Yeung J, Yaghoobi V, Miyagishima D, Vesely MD, Zhang T, Badri T, et al. Targeting the CSF1/CSF1R axis is a potential treatment strategy for malignant meningiomas. *Neuro Oncol* 2021;**23**:1922−35.
10. Cannarile MA, Weisser M, Jacob W, Jegg AM, Ries CH, Rüttinger D. Colony-stimulating factor 1 receptor (CSF1R) inhibitors in cancer therapy. *J Immunother Cancer* 2017;**5**:53.
11. Norden AD, Drappatz J, Wen PY. Novel anti-angiogenic therapies for malignant gliomas. *Lancet Neurol* 2008;**7**:1152−60.
12. Tanabe K, Wada J, Sato Y. Targeting angiogenesis and lymphangiogenesis in kidney disease. *Nat Rev Nephrol* 2020;**16**:289−303.
13. Gilbert MR, Dignam JJ, Armstrong TS, Wefel JS, Blumenthal DT, Vogelbaum MA, et al. A randomized trial of bevacizumab for newly diagnosed glioblastoma. *N Engl J Med* 2014;**370**:699−708.
14. Heffron TP. Small molecule kinase inhibitors for the treatment of brain cancer. *J Med Chem* 2016;**59**:10030−66.
15. Fu Y, Wei X, Lin L, Xu W, Liang J. Adverse reactions of sorafenib, sunitinib, and imatinib in treating digestive system tumors. *Thorac Cancer* 2018;**9**:542−7.
16. Schiff D, Jaeckle KA, Anderson SK, Galanis E, Giannini C, Buckner JC, et al. Phase 1/2 trial of temsirolimus and sorafenib in the treatment of patients with recurrent glioblastoma: north Central Cancer Treatment Group Study/Alliance N0572. *Cancer* 2018;**124**:1455−63.
17. Wenes M, Shang M, Di Matteo M, Goveia J, Martín-Pérez R, Serneels J, et al. Macrophage metabolism controls tumor blood vessel morphogenesis and metastasis. *Cell Metabol* 2016;**24**:701−15.
18. Larionova I, Kazakova E, Gerashchenko T, Kzhyshkowska J. New angiogenic regulators produced by TAMs: perspective for targeting tumor angiogenesis. *Cancers* 2021;**13**:3253.
19. Priceman SJ, Sung JL, Shaposhnik Z, Burton JB, Torres-Collado AX, Moughon DL, et al. Targeting distinct tumor-infiltrating myeloid cells by inhibiting CSF-1 receptor: combating tumor evasion of anti-angiogenic therapy. *Blood* 2010;**115**:1461−71.
20. Achyut BR, Shankar A, Iskander AS, Ara R, Angara K, Zeng P, et al. Bone marrow derived myeloid cells orchestrate antiangiogenic resistance in glioblastoma through coordinated molecular networks. *Cancer Lett* 2015;**369**:416−26.
21. Rao R, Han R, Ogurek S, Xue C, Wu LM, Zhang L, et al. Glioblastoma genetic drivers dictate the function of tumor-associated macrophages/microglia and responses to CSF1R inhibition. *Neuro Oncol* 2022;**24**:584−97.
22. Zhang T, Qu R, Chan S, Lai M, Tong L, Feng F, et al. Discovery of a novel third-generation EGFR inhibitor and identification of a potential combination strategy to overcome resistance. *Mol Cancer* 2020;**19**:90.
23. Ying W, Cheruku PS, Bazer FW, Safe SH, Zhou B. Investigation of macrophage polarization using bone marrow derived macrophages. *J Vis Exp* 2013;**76**:50323.
24. Liu Y, Gu Y, Han Y, Zhang Q, Jiang Z, Zhang X, et al. Tumor exosomal RNAs promote lung pre-metastatic niche formation by activating alveolar epithelial TLR3 to recruit neutrophils. *Cancer Cell* 2016;**30**:243−56.
25. Lv Y, Li M, Liu T, Tong L, Peng T, Wei L, et al. Discovery of a new series of naphthamides as potent VEGFR-2 kinase inhibitors. *ACS Med Chem Lett* 2014;**5**:592−7.
26. La DS, Belzile J, Bready JV, Coxon A, DeMelfi T, Doerr N, et al. Novel 2,3-dihydro-1,4-benzoxazines as potent and orally bioavailable inhibitors of tumor-driven angiogenesis. *J Med Chem* 2008;**51**:1695−705.
27. Meyers MJ, Pelc M, Kamtekar S, Day J, Poda GI, Hall MK, et al. Structure-based drug design enables conversion of a DFG-in binding CSF-1R kinase inhibitor to a DFG-out binding mode. *Bioorg Med Chem Lett* 2010;**20**:1543−7.
28. Wang Z, Peet NP, Zhang P, Jiang Y, Rong L. Current development of glioblastoma therapeutic agents. *Mol Cancer Therapeut* 2021;**20**:1521−32.
29. Würdinger T, Tannous BA. Glioma angiogenesis: towards novel RNA therapeutics. *Cell Adhes Migrat* 2009;**3**:230−5.
30. Garcia J, Hurwitz HI, Sandler AB, Miles D, Coleman RL, Deurloo R, et al. Bevacizumab (Avastin®) in cancer treatment: a review of 15 years of clinical experience and future outlook. *Cancer Treat Rev* 2020;**86**:102017.
31. Sanati M, Afshari AR, Amini J, Mollazadeh H, Jamialahmadi T, Sahebkar A. Targeting angiogenesis in gliomas: potential role of phytochemicals. *J Funct Foods* 2022;**96**:105192.
32. Cha GD, Kang T, Baik S, Kim D, Choi SH, Hyeon T, et al. Advances in drug delivery technology for the treatment of glioblastoma multiforme. *J Control Release* 2020;**328**:350−67.
33. Jackson CM, Choi J, Lim M. Mechanisms of immunotherapy resistance: lessons from glioblastoma. *Nat Immunol* 2019;**20**:1100−9.
34. Pombo Antunes AR, Scheyltjens I, Lodi F, Messiaen J, Antoranz A, Duerinck J, et al. Single-cell profiling of myeloid cells in glioblastoma across species and disease stage reveals macrophage competition and specialization. *Nat Neurosci* 2021;**24**:595−610.
35. Fu LQ, Du WL, Cai MH, Yao JY, Zhao YY, Mou XZ. The roles of tumor-associated macrophages in tumor angiogenesis and metastasis. *Cell Immunol* 2020;**353**:104119.
36. Khan MA, Assiri AM, Broering DC. Complement and macrophage crosstalk during process of angiogenesis in tumor progression. *J Biomed Sci* 2015;**22**:58.
37. Davis MI, Hunt JP, Herrgard S, Ciceri P, Wodicka LM, Pallares G, et al. Comprehensive analysis of kinase inhibitor selectivity. *Nat Biotechnol* 2011;**29**:1046−51.
38. Giles AJ, Hutchinson MND, Sonnemann HM, Jung J, Fecci PE, Ratnam NM, et al. Dexamethasone-induced immunosuppression: mechanisms and implications for immunotherapy. *J Immunother Cancer* 2018;**6**:51.
39. Kim JE, Patel MA, Mangraviti A, Kim ES, Theodros D, Velarde E, et al. Combination therapy with anti-PD-1, anti-TIM-3, and focal radiation results in regression of murine gliomas. *Clin Cancer Res* 2017;**23**:124−36.
40. Omuro A, Vlahovic G, Lim M, Sahebjam S, Baehring J, Cloughesy T, et al. Nivolumab with or without ipilimumab in patients with recurrent glioblastoma: results from exploratory phase I cohorts of CheckMate 143. *Neuro Oncol* 2018;**20**:674−86.
41. Reardon DA, Brandes AA, Omuro A, Mulholland P, Lim M, Wick A, et al. Effect of nivolumab *vs* bevacizumab in patients with recurrent glioblastoma: the CheckMate 143 phase 3 randomized clinical trial. *JAMA Oncol* 2020;**6**:1003−10.
42. Reardon DA, Kim TM, Frenel JS, Simonelli M, Lopez J, Subramaniam DS, et al. Treatment with pembrolizumab in programmed death ligand 1-positive recurrent glioblastoma: results from

the multicohort phase 1 KEYNOTE-028 trial. *Cancer* 2021;**127**: 1620−9.
43. Ries CH, Cannarile MA, Hoves S, Benz J, Wartha K, Runza V, et al. Targeting tumor-associated macrophages with anti-CSF-1R antibody reveals a strategy for cancer therapy. *Cancer Cell* 2014;**25**: 846−59.
44. Magkouta SF, Vaitsi PC, Pappas AG, Iliopoulou M, Kosti CN, Psarra K, et al. CSF1/CSF1R axis blockade limits mesothelioma and enhances efficiency of anti-PDL1 immunotherapy. *Cancers* 2021;**13**:2546.
45. Geindreau M, Ghiringhelli F, Bruchard M. Vascular endothelial growth factor, a key modulator of the anti-tumor immune response. *Int J Mol Sci* 2021;**22**:4871.
46. Song Y, Fu Y, Xie Q, Zhu B, Wang J, Zhang B. Anti-angiogenic agents in combination with immune checkpoint inhibitors: a promising strategy for cancer treatment. *Front Immunol* 2020;**11**:1956.
47. Yi M, Jiao D, Qin S, Chu Q, Wu K, Li A. Synergistic effect of immune checkpoint blockade and anti-angiogenesis in cancer treatment. *Mol Cancer* 2019;**18**:60.